

MEASUREMENTS IN ABLATING AIR  
TEFLON BOUNDARY LAYERS

John H. Chang and K.E. Center

AVCO EVERETT RESEARCH LABORATORY

RESEARCH REPORT 369  
SEPTEMBER 1971

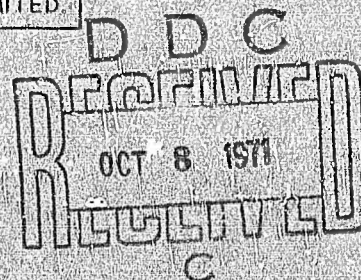
jointly sponsored by  
ADVANCED RESEARCH PROJECTS AGENCY  
DEPARTMENT OF DEFENSE  
ARPA Order #1052

and

SPACE AND MISSILE SYSTEMS ORGANIZATION  
AIR FORCE SYSTEMS COMMAND  
DEPUTY FOR RE-ENTRY SYSTEMS (RN)  
Norton Air Force Base, California 92409

APPROVED FOR PUBLIC RELEASE; DISTRIBUTION UNLIMITED

Reproduced by  
NATIONAL TECHNICAL  
INFORMATION SERVICE  
Springfield, Va 22151



Unclassified

Security Classification

## DOCUMENT CONTROL DATA - R&amp;D

(Security classification of title, body of abstract and indexing annotation must be entered when the overall report is classified.)

1 ORIGINATING ACTIVITY (Corporate author) Avco Everett Research Laboratory 2385 Revere Beach Parkway Everett, Massachusetts		2a REPORT SECURITY CLASSIFICATION Unclassified	
		2b GROUP	
3 REPORT TITLE  Measurements in Ablating Air Teflon Boundary Layers			
4 DESCRIPTIVE NOTES (Type of report and inclusive dates) Research Report 369			
5 AUTHOR(S) (Last name, first name, initial) Chang, John H. and Center, R. E.			
6 REPORT DATE September 1971		7a TOTAL NO. OF PAGES 23	7b NO. OF REFS 11
8a. CONTRACT OR GRANT NO. F04701-71-C-0033		8a. ORIGINATOR'S REPORT NUMBER(S)  Research Report 369	
b. PROJECT NO.			
c.		8b. OTHER REPORT NO(S) (Any other numbers that may be assigned this report) SAMSO-TR-71-144	
d.			
10. AVAILABILITY/LIMITATION NOTICES  Approved for Public Release; Distribution Unlimited			
11. SUPPLEMENTARY NOTES		12. SPONSORING MILITARY ACTIVITY Advanced Research Projects Agency, Department of Defense, ARPA Order #1092 and SAMSO, AFSC, Deputy for Re-entry Systems (RN), Norton Air Force Base, Cal. 92409.	
13. ABSTRACT → Theoretical descriptions of the detailed structure of ablating air-Teflon laminar boundary layer predict $CF_2$ to be a major constituent in the boundary layer. This species has not been observed experimentally. This paper presents spectrally and spatially resolved UV thermal radiation measurements which demonstrate the presence of $CF_2$ in the stagnation point boundary layer of ablating Teflon cylinder. The experiments were performed in an arc facility which provided subsonic air or nitrogen jets at 2500 to 4500°K and 1/40 atmospheric pressure. The state of the freestream was measured by the electron beam fluorescence technique. ( )			

DD FORM 1473  
1 JAN 64

Unclassified

Security Classification

14

## KEY WORDS

1. Ablating Boundary Layers
2. Air-Teflon Boundary Layer
3. CF<sub>2</sub> Emission Measurements
4. Low Density Arc

## LINK A

## LINK B

## LINK C

ROLE

WT

ROLE

WT

ROLE

WT

## INSTRUCTIONS

1. **ORIGINATING ACTIVITY:** Enter the name and address of the contractor, subcontractor, grantee, Department of Defense activity or other organization (corporate author) issuing the report.

2a. **REPORT SECURITY CLASSIFICATION:** Enter the overall security classification of the report. Indicate whether "Restricted Data" is included. Marking is to be in accordance with appropriate security regulations.

2b. **GROUP:** Automatic downgrading is specified in DoD Directive 5200.10 and Armed Forces Industrial Manual. Enter the group number. Also, when applicable, show that optional markings have been used for Group 3 and Group 4 as authorized.

3. **REPORT TITLE:** Enter the complete report title in all capital letters. Titles in all cases should be unclassified. If a meaningful title cannot be selected without classification, show title classification in all capitals in parenthesis immediately following the title.

4. **DESCRIPTIVE NOTES:** If appropriate, enter the type of report, e.g., interim, progress, summary, annual, or final. Give the inclusive dates when a specific reporting period is covered.

5. **AUTHOR(S):** Enter the name(s) of author(s) as shown on or in the report. Enter last name, first name, middle initial. If military, show rank and branch of service. The name of the principal author is an absolute minimum requirement.

6. **REPORT DATE:** Enter the date of the report as day, month, year, or month, year. If more than one date appears in the report, use date of publication.

7a. **TOTAL NUMBER OF PAGES:** The total page count should follow normal pagination procedures, i.e., enter the number of pages containing information.

7b. **NUMBER OF REFERENCES:** Enter the total number of references cited in the report.

8a. **CONTRACT OR GRANT NUMBER:** If appropriate, enter the applicable number of the contract or grant under which the report was written.

8b, 8c, & 8d. **PROJECT NUMBER:** Enter the appropriate military department identification, such as project number, subproject number, system numbers, task number, etc.

9a. **ORIGINATOR'S REPORT NUMBER(S):** Enter the official report number by which the document will be identified and controlled by the originating activity. This number must be unique to this report.

9b. **OTHER REPORT NUMBER(S):** If the report has been assigned any other report number(s) (either by the originator or by the sponsor), also enter this number(s).

10. **AVAILABILITY LIMITATION NOTICES:** Enter any limitations on further dissemination of the report, other than those

imposed by security classification, using standard statements such as:

- (1) "Qualified requesters may obtain copies of this report from DDC."
- (2) "Foreign announcement and dissemination of this report by DDC is not authorized."
- (3) "U. S. Government agencies may obtain copies of this report directly from DDC. Other qualified DDC users shall request through \_\_\_\_\_."
- (4) "U. S. military agencies may obtain copies of this report directly from DDC. Other qualified users shall request through \_\_\_\_\_."
- (5) "All distribution of this report is controlled. Qualified DDC users shall request through \_\_\_\_\_."

If the report has been furnished to the Office of Technical Services, Department of Commerce, for sale to the public, indicate this fact and enter the price, if known.

11. **SUPPLEMENTARY NOTES:** Use for additional explanatory notes.

12. **SPONSORING MILITARY ACTIVITY:** Enter the name of the departmental project office or laboratory sponsoring (paying for) the research and development. Include address.

13. **ABSTRACT:** Enter an abstract giving a brief and factual summary of the document indicative of the report, even though it may also appear elsewhere in the body of the technical report. If additional space is required, a continuation sheet shall be attached.

It is highly desirable that the abstract of classified reports be unclassified. Each paragraph of the abstract shall end with an indication of the military security classification of the information in the paragraph, represented as (TS), (S), (C), or (U).

There is no limitation on the length of the abstract. However, the suggested length is from 150 to 225 words.

14. **KEY WORDS:** Key words are technically meaningful terms or short phrases that characterize a report and may be used as index entries for cataloging the report. Key words must be selected so that no security classification is required. Identifiers, such as equipment model designation, trade name, military project code name, geographic location, may be used as key words but will be followed by an indication of technical or text. The assignment of links, rules, and weights is optional.

MEASUREMENTS IN ABLATING AIR TEFLON BOUNDARY LAYERS

by

John H Chang\* and R. E. Center

AVCO EVERETT RESEARCH LABORATORY  
a division of  
AVCO CORPORATION  
Everett, Massachusetts

Contract F04701-71-C-0033

September 1971

jointly sponsored by

ADVANCED RESEARCH PROJECTS AGENCY  
DEPARTMENT OF DEFENSE  
ARPA Order #1092

and

SPACE AND MISSILE SYSTEMS ORGANIZATION  
AIR FORCE SYSTEMS COMMAND  
DEPUTY FOR RE-ENTRY SYSTEMS (RN)  
Norton Air Force Base, California 92409

Approved for Public Release; Distribution Unlimited

---

\*Fluid Mechanics Laboratory, TRW Systems Group, One Space Park,  
Redondo Beach, California 90278

## FOREWORD

Approved for Public Release; Distribution Unlimited

This research was supported by the Advanced Research Projects Agency of the Department of Defense and Space and Missile Systems Organization, Air Force Systems Command under Contract F04701-71-C-0033. This work was initiated under a previous contract. The secondary report number as assigned by AERL is Avco Everett Research Laboratory Research Report 369. The Air Force program monitor for this contract is Capt. M. Anderson, USAF, Project Officer, Environmental Technology Branch, RNSE.

Publication of this report does not constitute Air Force approval of the report's findings or conclusions; it is published only for the exchange and stimulation of ideas.

Capt. M. Anderson  
Project Officer  
Environmental Technology Branch  
RNSE

## ABSTRACT

Theoretical descriptions of the detailed structure of ablating air-Teflon laminar boundary layer predict  $\text{CF}_2$  to be a major constituent in the boundary layer. This species has not been observed experimentally. This paper presents spectrally and spatially resolved UV thermal radiation measurements which demonstrate the presence of  $\text{CF}_2$  in the stagnation point boundary layer of ablating Teflon cylinder. The experiments were performed in an arc facility which provided subsonic air or nitrogen jets at 2500 to 4500°K and 1/40 atmospheric pressure. The state of the freestream was measured by the electron beam fluorescence technique.

## TABLE OF CONTENTS

	Foreword	ii
	Abstract	iii
I.	INTRODUCTION	1
II.	EXPERIMENTAL APPARATUS	3
III.	EXPERIMENTAL RESULTS	7
IV.	CONCLUSION	21
	ACKNOWLEDGMENT	22
	References	23

## I. INTRODUCTION

The detailed structure of laminar ablating air-Teflon boundary layers has been the subject of many investigations.<sup>(1-4)</sup> Most of the experimental data has been reviewed in Ref. 3, which includes an analysis developed to describe the structure of the boundary layer. The analysis uses a partial equilibrium model for the air-Teflon chemistry which does not permit the formation of  $\text{CF}_3$  and  $\text{CF}_4$  within the boundary layer. The validity of the model was based on the excellent agreement between the measured and the theoretically predicted peak intensity of  $\text{CO}_2$  radiation, its position in the boundary layer and the integrated intensity across the boundary layer. This theory further predicts the presence of  $\text{COF}_2$  as a major radiator in air-Teflon boundary layers. Measurements of absolute intensities by Young, et al,<sup>(4)</sup> were in good agreement with theoretical predictions. The analysis also predicts that  $\text{CF}_2$  would be a major species in the boundary layer. This species has not been experimentally observed.

The work presented here was undertaken to demonstrate the existence of  $\text{CF}_2$  in the air-Teflon boundary layers by spectrally resolved UV thermal radiation measurements in the stagnation point boundary layer of ablating Teflon cylinders. After demonstrating its presence, the spatial distribution of the  $\text{CF}_2$  emission in the boundary layer was measured in order to provide additional information on the chemical processes in the boundary layer. A low density DC arc jet facility was used to provide subsonic air or nitrogen jets at  $2500^\circ\text{K}$  to



4500°K and 1/40 atmospheric pressure. The state of the freestream gas was measured by use of an electron beam probe. The boundary layer measurements were made at the stagnation point of a 1 cm diameter by 1 cm long Teflon cylinder. By measuring on the axis of the jet, the problems of interference by the jet's mixing boundaries, the cold nozzle wall boundary layers and other jet nonuniformities were eliminated. In addition the stagnation point provided both a laminar boundary layer and sufficient heat transfer for steady state ablation to be rapidly reached over a wide range of arc operating conditions.

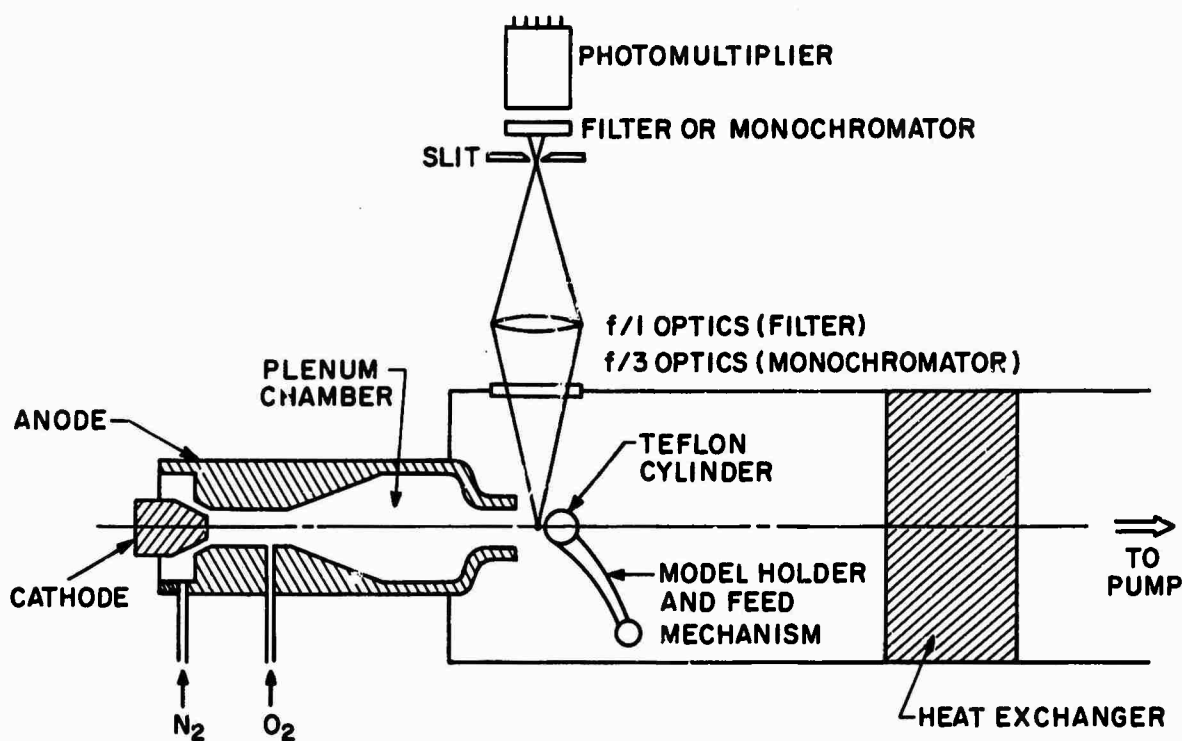
## II. EXPERIMENTAL APPARATUS

### A. Arc Jet

The AERL low density arc jet is a D. C. battery powered facility which produces a subsonic air jet at temperatures from 2500°K to 4500°K and at a pressure of 1/40 atmosphere. The input power is variable over the range of 30 to 80 kw. The air mass flow was approximately 1.5 gms/sec and the flow velocity was  $10^5$  cm/sec. A schematic diagram of the arc is presented in Fig. 1. Nitrogen is introduced around the circumference of the 2% thoriated tungsten cathode. It flows around the cathode and into the anode section. This swirling flow stabilizes the arc by constricting the arc to the anode centerline. Oxygen is introduced downstream of the anode by means of twelve radial holes circumferentially placed at the entrance to the plenum chamber. The gases mix within the plenum chamber and the hot air exits through the 1.9 cm diameter nozzle. All internal components are water cooled, and with the exception of the cathode, are constructed of copper. The arc is enclosed in the low pressure chamber which is evacuated by a 500 cfm pumping system using a Stokes mechanical pump.

The gas power was determined by subtracting the wall losses from the arc input power. These losses were obtained by measuring the temperature rise  $\Delta T$  and the flow rate of the coolant water,  $\dot{m}_{H_2O}$ , through the arc. The enthalpy per unit mass of gas,  $H$ , was then given by

$$H = \frac{VI - \dot{m}_{H_2O} \Delta T}{\dot{m}_{air}} \quad (1)$$



C6959

Fig. 1 Schematic of low density arc jet and associated optical system.

where  $V$  and  $I$  are the arc operating voltage and current respectively and  $S$  is the specific heat of water. Assuming the gas to be in thermochemical equilibrium, an energy balance temperature for the gas can be directly deduced from the above calculated enthalpy.

#### B. The Model Holder and Injection Mechanism

The model holder was designed to move the Teflon cylinder into the jet after steady state conditions had been obtained in the operation of the arc. This was done to avoid severe ablation of the Teflon cylinder during the time taken for the cooling system to reach steady state, approximately 7 seconds. For the spectral scans of the ablating boundary layer it was necessary to maintain the entrance slit of the monochromator focused at a fixed point relative to the cylinder. Therefore, a model holder was equipped with a variable speed motor drive which mechanically fed the cylinder toward the arc nozzle exit at the same rate as the measured ablation rate.

#### C. The Spectrometric System

The optical system is shown schematically in Fig. 1. For the freestream density measurements an  $f/1$  Cassagrain optical system with an S-13 photomultiplier detector was used to measure the electron beam excited fluorescence through selected narrow band pass filters. The species concentration and boundary layer measurements were made with an  $f/3$  reflecting optical system which directed the emission to a Jarrell Ash Elbert 0.25 meter double pass grating monochromator. The resolution along the jet axis was 0.140 mm when using a  $100\mu$  monochromator entrance slit. This slit width gave a triangular spectral resolution function with a full width at half height of  $3.2 \text{ \AA}$ .

For the spectral measurements from 2000 to 5500 Å the emission signal was detected by an S-13 photomultiplier. A photomultiplier with an S-20 surface was used for spectral measurements in the range of 5000 to 8000 Å. The photomultiplier signals were displayed on an X-Y recorder. The optical windows were all made of quartz. The optical, detector and recording system was calibrated as a unit by use of a tungsten lamp with its filament located on the arc axis at the model location.

#### D. Electron Beam

The electron gun produced about 80 keV energy electrons which entered the arc test chamber through a drift tube with 1.75 mm diameter exit orifice. The electron beam was directed normal to the arc jet and intersected the jet centerline 1.27 cm downstream of the nozzle exit. The beam current which was variable from 0 to 250  $\mu$  amps was measured by a shielded Faraday cage. For the experiments in hot air jets, the presence of freestream plasma can influence the current values measured by the Faraday cage. To prevent interference of the Faraday cage signal by the freestream plasma, a thin aluminum foil (0.01 mm thickness) was placed over the entrance of the cage. The collector was connected directly to an oscilloscope and the signal monitored throughout an experiment. The grid of the electron gun was pulsed at 50% duty cycle to permit the use of phase sensitive detection, thus minimizing the contribution of background thermal radiation during the electron fluorescence measurements. The duration of the electron beam pulse could be varied between 200  $\mu$  sec and 10 msec.

### III. EXPERIMENTAL RESULTS

#### A. Freestream Density Measurements

The use of the electron beam fluorescence technique has been described elsewhere.<sup>(5)-(7)</sup> The molecular nitrogen density was determined from emission intensity measurements of the  $N_2$  second positive system,  $C^3\Pi \rightarrow B^3\Pi$ . This transition was chosen rather than the first negative system because of the large collision quenching cross section<sup>(8)</sup> for the  $B^2\Sigma$  state of  $N_2^+$  by ground state  $N_2$ . The collision quenching rate of the  $N_2(2+)$  system by  $N_2$  is two orders of magnitude smaller than the corresponding rate for the  $N_2^+(1-)$  system. In air the quenching rate is determined by the oxygen concentration. The rate constants experimentally determined by Brocklehurst<sup>(8)</sup> indicate that quenching of the second positive system should not be important for air densities less than  $10^{17}/\text{cm}^3$ , and this was verified experimentally.

Figure 2 shows some oscillographs of the photomultiplier and beam current signals for the beam excited radiation from the  $N_2(2+)$  system at various arc input power levels. A  $3370 \text{ \AA}$  interference filter with a half width of  $140 \text{ \AA}$  was used to isolate the second positive system. The electron beam current was simultaneously measured by the shielded Faraday cage, and the output is displayed with the optical signal on the lower beam of the dual beam oscilloscope. From the magnitude of the photomultiplier output when the electron beam is off, one can observe that the signal due to thermal radiation was negligible compared to the electron fluorescence. Since the diffusion of the secondary electrons

NOT REPRODUCIBLE

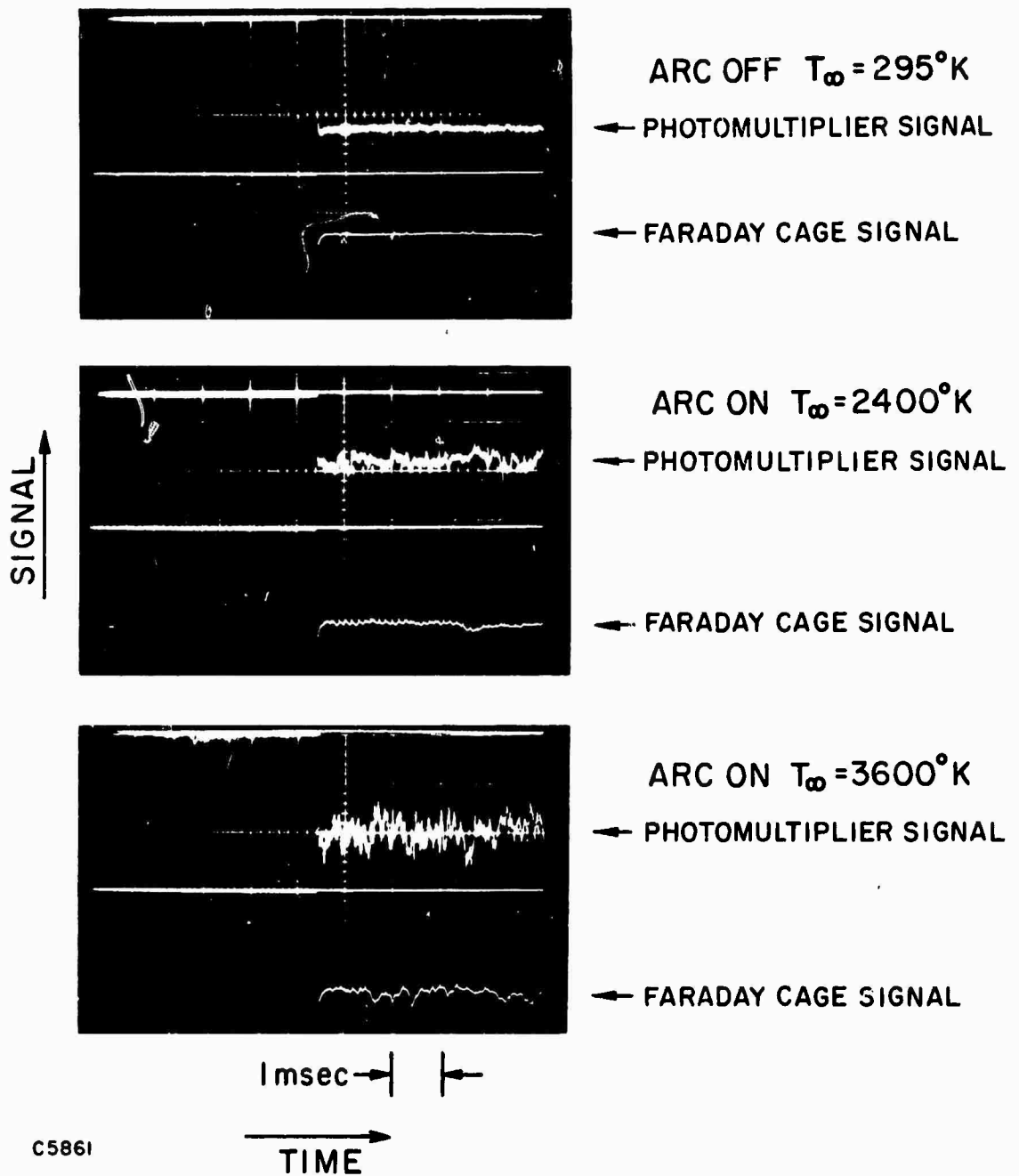


Fig. 2 Electron beam current and photomultiplier response to the  $\text{N}_2(2+)$  emission at the jet centerline. The electron beam was chopped at 100 Hz with a 50% duty cycle.

from the main beam is small at these pressures, the spatial resolution of the optical system was determined by the electron beam diameter and the limiting slit dimension in the system. Furthermore, the upper state of the  $N_2(2+)$  system has a lifetime of  $2.7 \times 10^{-8}$  seconds, which is small compared to the characteristic flow times for a flow velocity of  $10^5$  cm/sec in the jet. These two factors permit the local measurements of density and density fluctuations in the jet. Over the range of jet gas temperature from  $2400^\circ\text{K}$  to  $3600^\circ\text{K}$ , the measured gas density agreed to within 10 percent with the magnitude deduced from the arc energy balance temperature and the measured pressure.

The response time of the fluorescence detection and recording system was  $10^{-4}$  second, thus permitting measurement of density fluctuations up to 10 KHz in the arc jet. Measurements at comparable intensities with cold jets indicated no observable fluctuation in the electron beam system. Therefore, estimates of the point density fluctuation could be made from the measured fluctuations in the electron fluorescence signals for the hot jets. From results similar to those shown in Fig. 2, maximum density fluctuations of  $\pm 10$  percent peak to peak were observed for a range of jet temperatures between 2400 to  $3600^\circ\text{K}$ .

The radial density profile of the jet was measured by monitoring the  $N_2(2+)$  electron excited fluorescence as the optical system was traversed along the electron beam, i. e., across the jet. The results of such a scan for the case of  $2800^\circ\text{K}$  freestream are shown in Fig. 3. The effects of collisional quenching with oxygen concentration have been



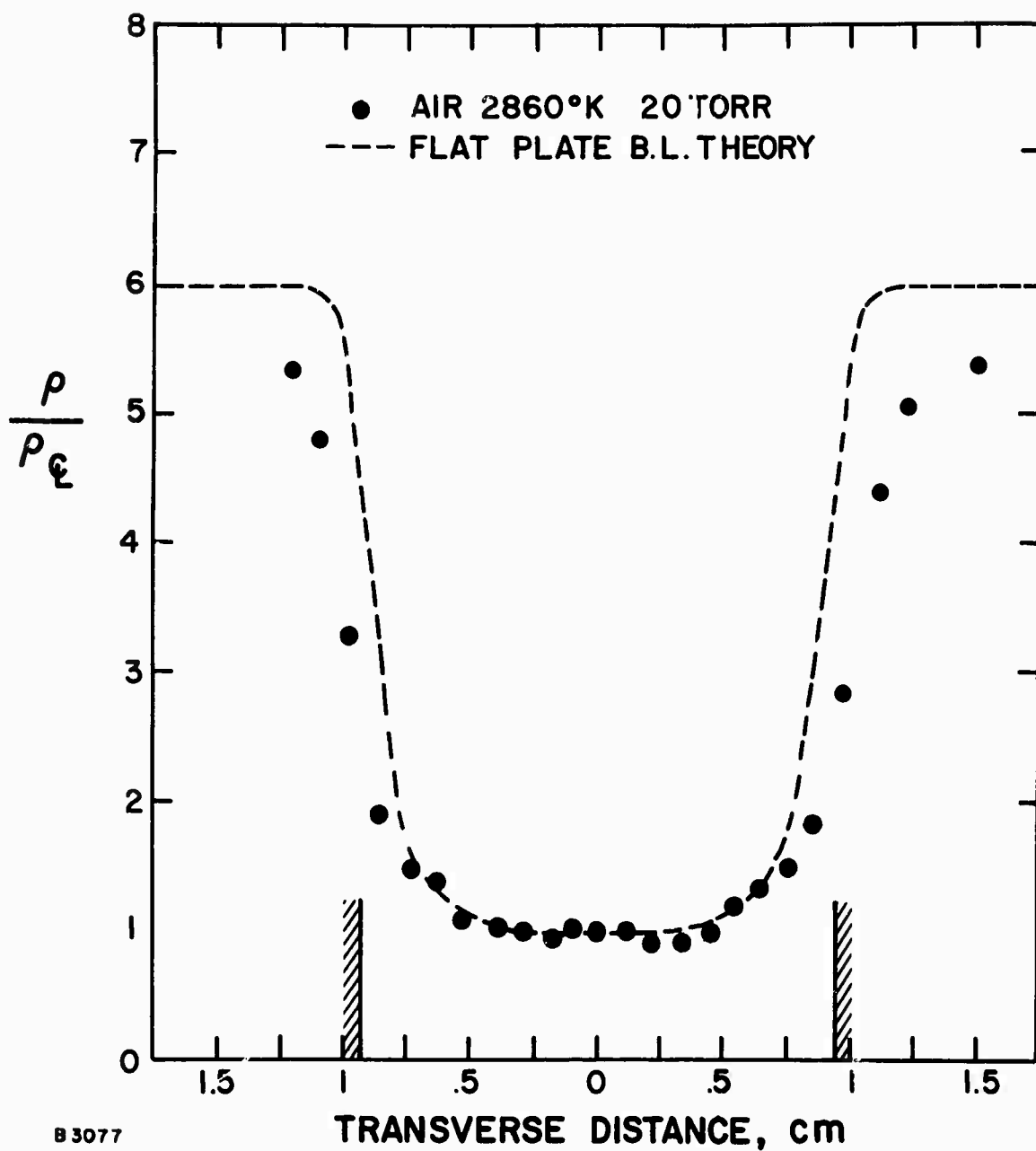


Fig. 3 Measurement of the radial density profile in the arc jet.

folded into the data points. Also shown in Fig. 3 is the theoretical density profile predicted from flat plate equilibrium boundary layer calculations for the same nozzle exit conditions. The effect of finite optical aperture has been included in the calculated profile. The experimental results show a constant density core of approximately 1.5 cm for the arc conditions of interest. This limited the cylinder dimension to 1 cm long by 1 cm in diameter.

## B. Thermal Radiation Measurement in Teflon-Air Boundary Layer

### 1. Detection of $CF_2$

To investigate the presence of  $CF_2$  in the ablating Teflon boundary layer, UV thermal radiation spectra were taken at the stagnation point of the ablating Teflon cylinder. For the spectral scans the entrance slit of the monochromator, 0.1 mm, was focused at a fixed point relative to the ablating cylinder throughout the measurement. This was accomplished by mechanically feeding the cylinder at the same rate as the measured steady state ablation rates. The time to reach steady state ablation was measured to be 2 seconds for the 2600°K freestream temperature and less than  $\frac{1}{2}$  second for the 3500°K freestream temperature. Following this incubation time, the ablation rate at a given freestream temperature was observed to be constant until the cylinder diameter had been reduced by more than 40%. The measured ablation rates were 0.056 mm/sec, 0.125 mm/sec, and 0.17 mm/sec for the freestream temperature of 2600°K, 2850°K and 3500°K.

For a given ablation rate the range of wavelength which could be covered by the scanning monochromator depended upon the monochromator scanning rate and the maximum tolerable change in the radius of curvature.

The monochromator was scanned at  $16 \text{ \AA/sec}$ . For the freestream temperature of  $2600^\circ\text{K}$ , a scan of  $400 \text{ \AA}$  could be covered while the cylinder diameter decreased by 10 percent of its original dimension. Therefore, the entire wavelength range for the expected  $\text{CF}_2$  radiation was covered by a composite of runs at the same freestream condition. The wavelength range of consecutive runs was overlapped to determine the effect of the variations in the radius of curvature of the model.

Figure 4 shows a composite of the recorded photomultiplier output for wavelength range of  $2400 \text{ \AA}$  to  $3700 \text{ \AA}$  for a freestream temperature of  $2600^\circ\text{K}$ . The monochromator entrance slit of  $100 \mu$  resulted in a spectral resolution of  $3.2 \text{ \AA}$  and a spatial resolution of  $0.140 \text{ mm}$ . The wavelength scan was initiated 10 seconds after the cylinder was introduced into the freestream to ensure that steady state ablation had been achieved. The overlapping of the wavelength between consecutive runs indicated that the variation of radius of curvature of the cylinder had a negligible effect on the magnitude of the emission intensity. The  $\text{N}_2(2+)[0,0]$  band head and the atomic nitrogen lines serve as an internal check on the wavelength calibration during the experiment. Also shown in Fig. 4 are the wavelength location for  $\text{CF}_2$  emission band heads as identified by Venkateswarlu. <sup>(9)</sup> The observed spectra demonstrate the presence of  $\text{CF}_2$  in the air Teflon boundary layer. Similar spectra were obtained for freestream temperatures of  $2860^\circ\text{K}$  and  $3500^\circ\text{K}$ .

The boundary layer theory of Ref. 3 also predicts that  $\text{COF}_2$  should be present in the air-Teflon boundary close to the body with a

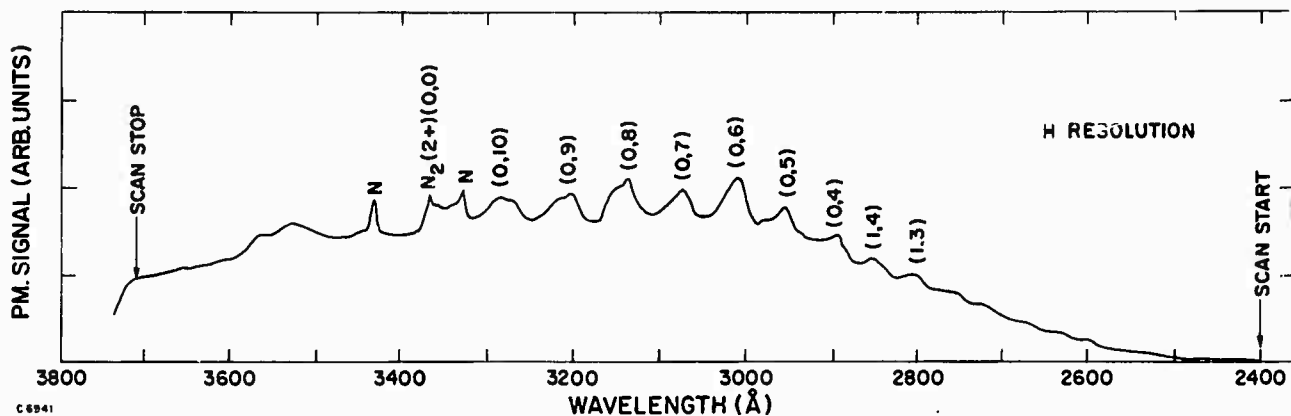


Fig. 4 Composite spectral scan of the thermal emission in the air-Teflon boundary layer for  $T_{\infty} = 2600^{\circ}\text{K}$ . The optical slit was focused 0.1 mm in front of the stagnation point and the spectral resolution was  $3.2 \text{ \AA}$ .

similar concentration to that of  $\text{CF}_2$ . Young et al<sup>(4)</sup> have observed IR emission from  $\text{COF}_2$  in the air-Teflon boundary layer. Since  $\text{COF}_2$  can also radiate in the UV, experiments were conducted to verify that the observed radiation was  $\text{CF}_2$  rather than  $\text{COF}_2$ . Similar spectral scans were carried out with decreasing oxygen content in the heated jet.

Figure 5 shows a spectrum for a pure nitrogen jet with power setting such that the ablation rate is similar to that of the  $2600^\circ\text{K}$  air jet. Only ablation rates were matched because the nitrogen jet was not in thermochemical equilibrium and therefore comparison of the freestream parameters is not meaningful. For equivalent ablation rates, the spectra observed were sufficiently similar in intensity and character for both air and nitrogen jets to confirm that the observed radiation was due to  $\text{CF}_2$  and not  $\text{COF}_2$ .

The entire optical, electronic, recording system and the monochromator was calibrated with a tungsten lamp of known temperature. Thus, the absolute intensity of the observed radiation could be directly obtained from the photomultiplier output with the aid of the spectral calibration curves. The contribution of the background radiation and surface reflection was estimated by substituting the Teflon cylinder with a polished copper cylinder of the same size. In the wavelength regime where the  $\text{CF}_2$  emission was observed, the radiation with the nonablating copper cylinder was negligible compared to that measured with the ablating cylinders.

## 2. Spatial Distribution Measurement

To determine the  $\text{CF}_2$  concentration profile in the boundary layer, spatially resolved measurements of the absolute intensity were

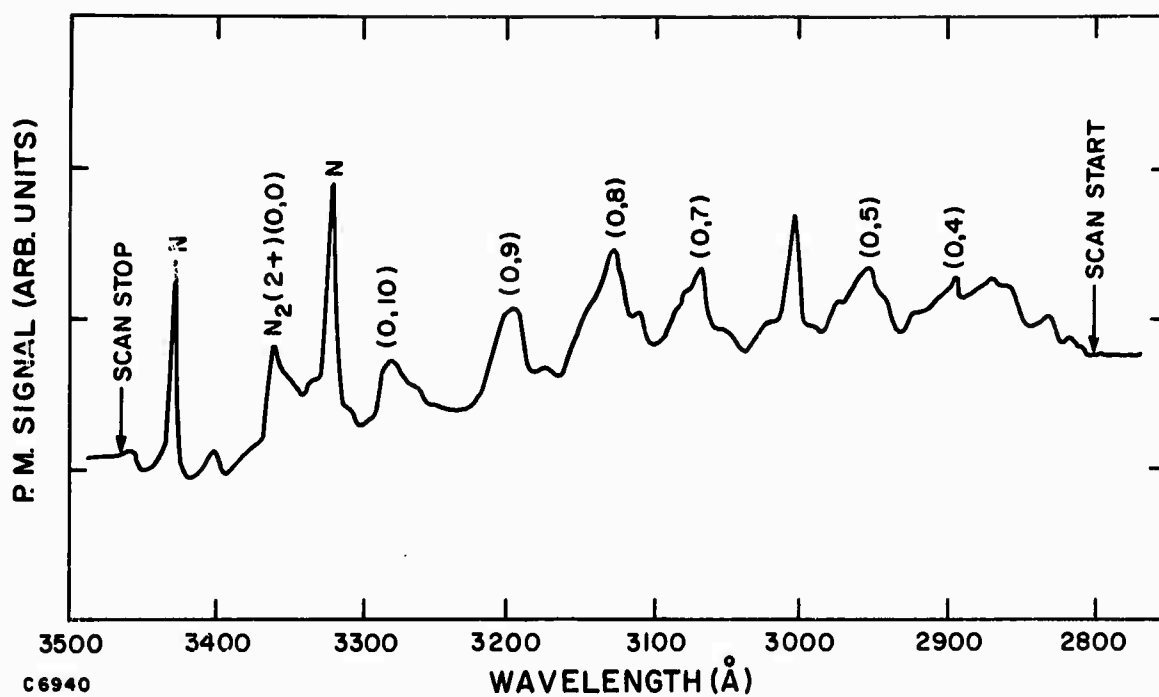


Fig. 5 Composite spectral scan of the thermal emission in the N<sub>2</sub>-Teflon boundary layer for the same ablation rate as in Fig. 4.

made with the monochromator set at  $3075 \pm 1.6 \text{ \AA}$  to monitor the  $\text{CF}_2$  (0, 7) system. The imaged slit width at the body was 0.14 mm. The profiles were obtained by fixing the slit image location and allowing the cylinders to ablate at a known rate. The measured intensity profiles for freestream temperatures of  $2600^\circ\text{K}$  and  $3500^\circ\text{K}$  are presented in Fig. 6. The concentration profiles of  $\text{CF}_2$  and  $\text{COF}_2$  predicted by the partial equilibrium theory of Greenberg, et al, <sup>(3)</sup> are presented in Fig. 7. In this theory, the laminar boundary layer equations are coupled to the Teflon surface through heat and mass balances, using a constant ablation temperature of  $1000^\circ\text{K}$  for Teflon. Chemical nonequilibrium effects are taken into account by a partial equilibrium chemistry model, which does not allow the formation of  $\text{CF}_3$  and  $\text{CF}_4$ . The external flowfield for the cylindrical geometry was properly incorporated but the azimuthal pressure gradient in the boundary layer was neglected in these preliminary calculations. The individual transport properties of all the elements were set equal and all Lewis and Prandtl numbers were taken as unity. The measured profiles show good spatial agreement with the predicted profile.

The partial equilibrium theory predicts that the  $\text{CF}_2$  exists close to the surface in the region of relatively low temperature. The calculated profiles for freestream temperatures of  $2600$  and  $3300^\circ\text{K}$  are shown in Fig. 8. The peak of the observed  $\text{CF}_2$  fluorescence coincides approximately with calculated temperatures of  $1800^\circ\text{K}$  as seen from Figs. 6 and 8. Comparison of the observed emission with that based on the available f numbers for  $\text{CF}_2$  <sup>(10, 11)</sup> and the calculated

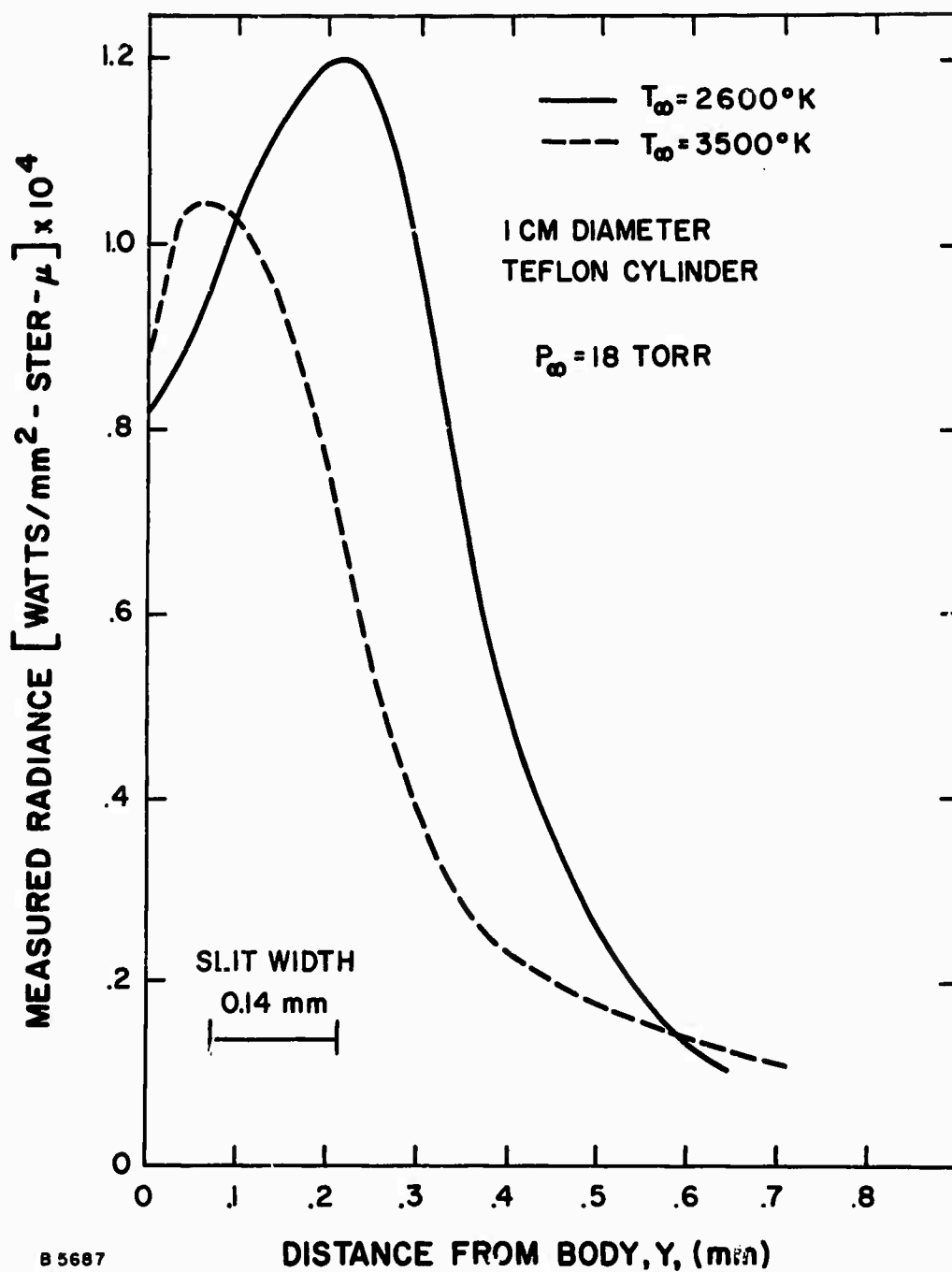


Fig. 6  $\text{CF}_2$  concentration profile measurements.



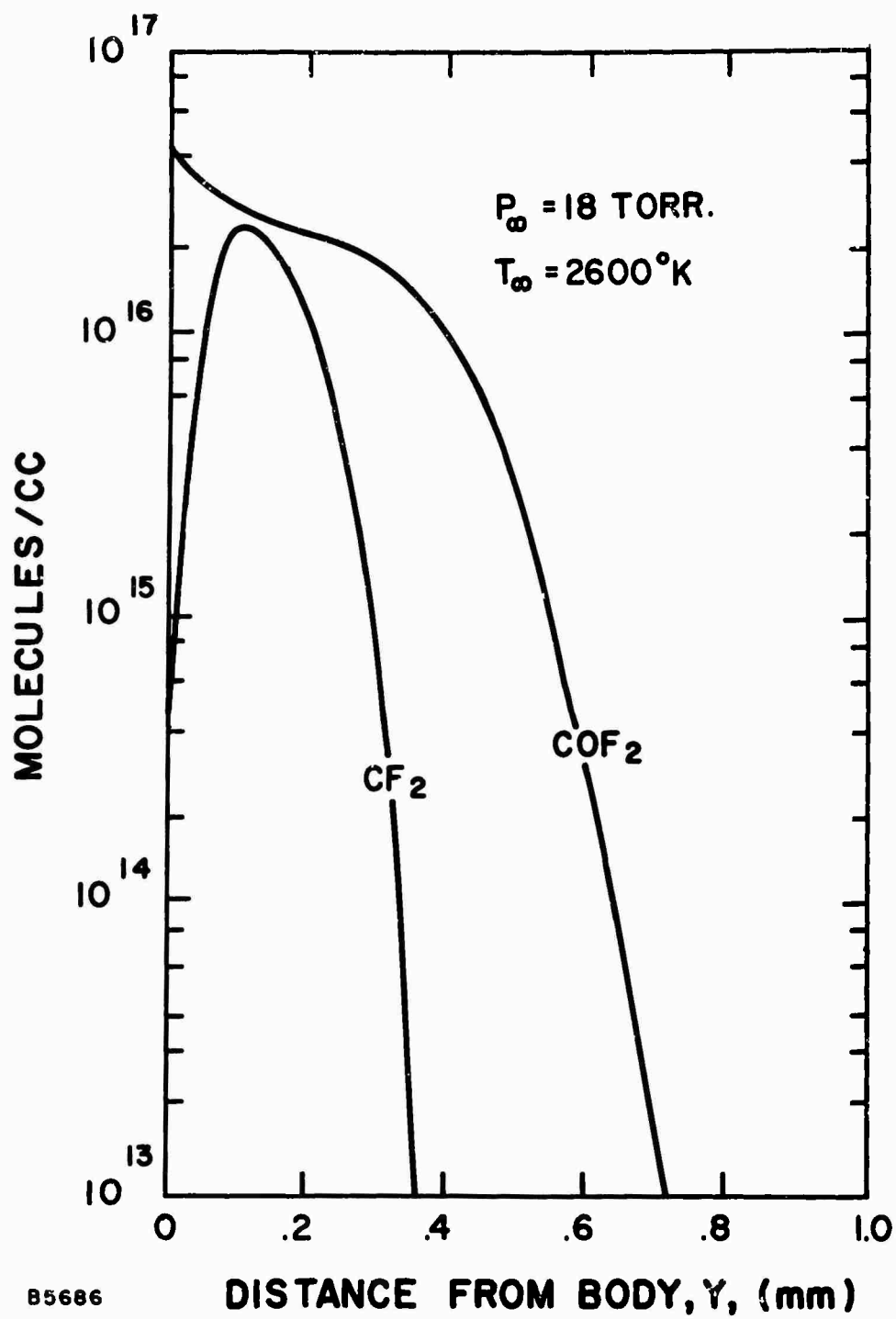


Fig. 7 Theoretical  $\text{CF}_2$  and  $\text{COF}_2$  concentration profiles.

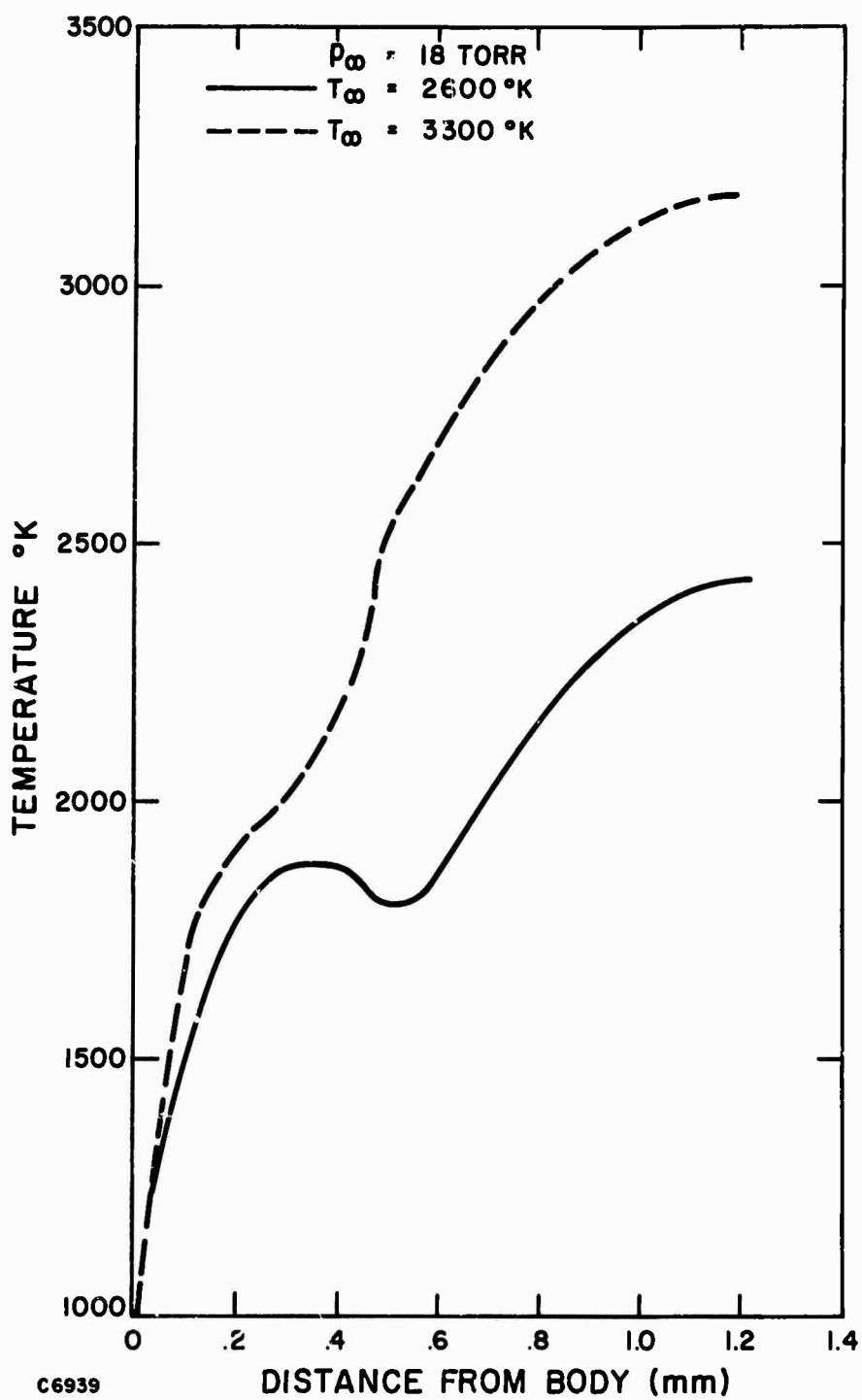


Fig. 8 Theoretical temperature profiles in the air-Teflon stagnation point boundary layer.

temperature and concentration profiles indicate that the observed radiation was approximately two orders of magnitude larger than predicted. This discrepancy may result from the chemiluminescent reaction  $CF + F \rightarrow CF_2 + h\nu$  or some nonequilibrium processes in the boundary layer.

#### IV. CONCLUSION

Spectrally and spatially resolved UV radiation measurements at the stagnation point of an ablating Teflon cylinder have confirmed the existence of  $\text{CF}_2$  in the air-Teflon boundary layer. The spatially resolved profiles of the absolute radiation intensity of the  $\text{CF}_2$  (0, 7) emission at  $3075 \text{ \AA}$  showed the  $\text{CF}_2$  to be concentrated near the ablating body. Good spatial agreement exists between the measured and predicted  $\text{CF}_2$  concentration profiles. The magnitude of the observed radiation intensity is approximately two orders to magnitude greater than that calculated from available f numbers and the predicted concentration. This large discrepancy in radiation may suggest the possibility of chemiluminescent reaction such as  $\text{CF} + \text{F} \rightarrow \text{CF}_2 + h\nu$  or some nonequilibrium processes in the air-Teflon mixture. It must be pointed out that the theory employed is the simplest which contains the relevant chemistry. The assumption of the absence of  $\text{CF}_3$  and  $\text{CF}_4$  may not be applicable at these pressure levels.

The state of the freestream gas was measured by the electron beam fluorescence technique. The gas densities deduced from the magnitude of the electron luminescence of the  $\text{N}_2$  (2+) system agreed within 10% with those deduced from arc energy balance temperatures and measured pressure. The point density fluctuation in the jet was measured to be of the order  $\pm 10\%$  of the mean.

## ACKNOWLEDGMENT

The authors enjoyed many stimulating discussions with Dr. Morton Camac. The identification of the  $\text{CF}_2$  spectra was carried out by Dr. Lee Young. The authors are also grateful to Mr. R. Rennie for his assistance in the operation of the arc facility.

## REFERENCES

1. Wray, K. L., Rose, P. H., and Koritz, H. E., "Measurements of the Radiation from an Ablation Contaminated Boundary Layer under Simulated Flight Conditions," AERL Research Report 226 (August 1965).
2. Wray, K. L. and Kemp, N. H., "The Ablating Boundary Layer on a Teflon Plate in an Arc Heated Air-Teflon Stream," AIAA Paper No. 66-56 (January 1966).
3. Greenberg, R. A., Kemp, N. H., and Wray, K. L., "Structure of the Laminar Ablating Air-Teflon Boundary Layer," AIAA Journal, Vol. 8, p. 619 (April 1970).
4. Young, L. A., Greenberg, R. A., and Wray, K. L., "COF<sub>2</sub> Radiation from an Ablating Air-Teflon Boundary Layer," J. Quant. Spectrosc. Radiat. Transfer 10, p. 189 (1970).
5. Camac, M., "Boundary Layer Measurements with an Electron Beam," AERL Research Report 275 (July, 1967).
6. Muntz, E. P. and Marsden, D. J., "Electron Excitation Applied to Experimental Investigation of Rarefied Gas Flow," Rarefied Gas Dynamics, Vol. II, pp 495-526, Academic Press, 1963.
7. Schumacher, B. and Gadamer, E., "Electron Beam Fluorescence Probe for Measuring the Local Gas Density in a Wide Field of Observation," Canadian Journal of Physics, Vol. 36, p. 659 (1958).
8. Brocklehurst, B., "Luminescence of Gases Excited by High Energy Radiation, Part I, Collisional Deactivation in Nitrogen," Trans. Faraday Soc. 60, p. 2151, (1964).
9. Venkateswarlu, P., "On the Emission Bands of CF<sub>2</sub>," Phys. Review 77, 676 (1950).
10. Modica, A. P., "Electronic Oscillator Strength of CF<sub>2</sub>," J. Phys. Chem. 72, p. 4594, (1968).
11. Hooker, W. J. and Sellers, R. P., "The Absorption Spectra of Shock Heated Teflon/Argon and Teflon/Nitrogen Mixtures," AMRAC Proceedings, Vol. XIII, Part I, (November, 1969).